Expanded View Figures

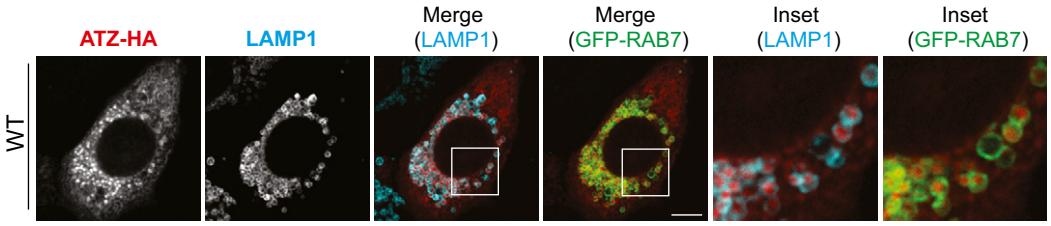

Figure EV1. Endolysosomes display LAMP1 and GFP-RAB7 at the limiting membrane.

CLSM analysis showing LAMP1 (cyan) and GFP-RAB7 (green) co-localization at the limiting membrane of endolysosomes containing ATZ-HA (red). Scale bar: 10 μm.

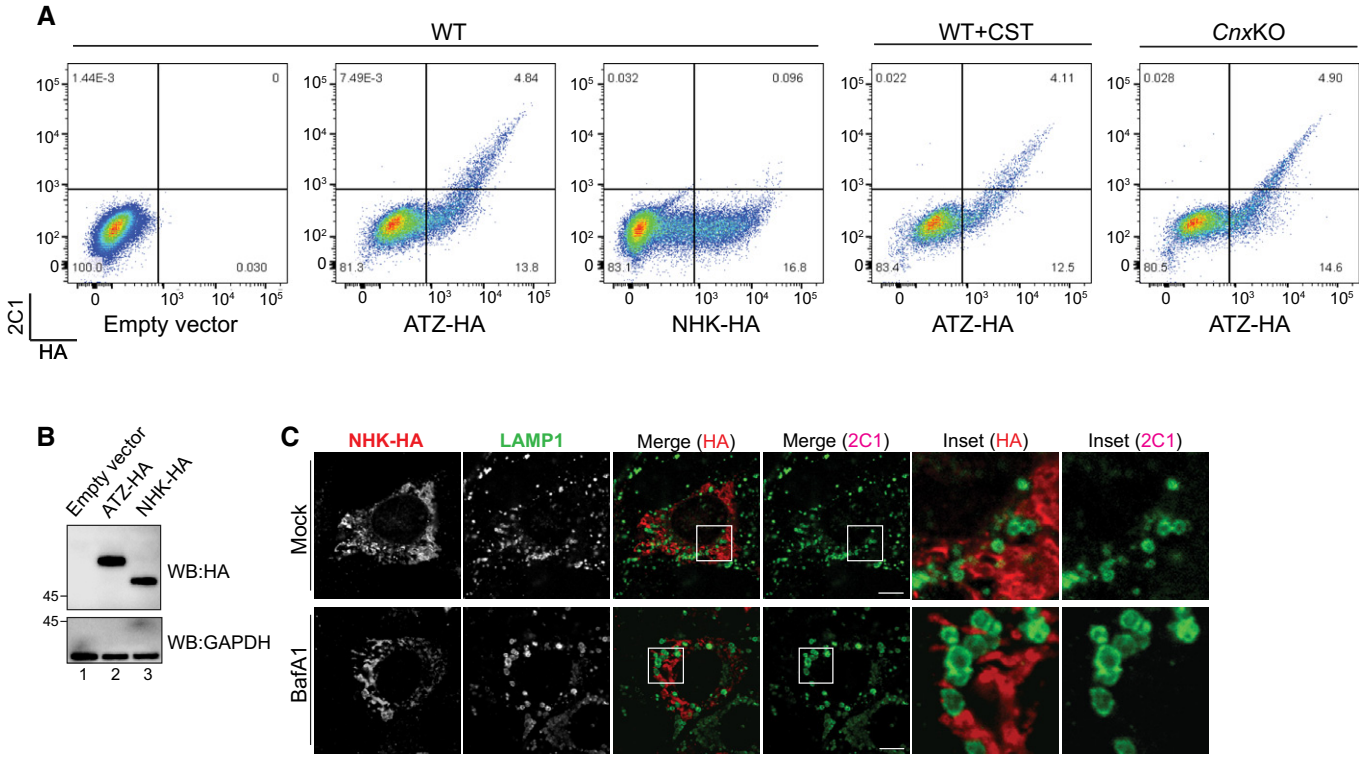

Figure EV2. ATZ, but not NHK, forms 2C1-positive polymers.

A Flow cytofluorimetric analyses to assess HA (*x*-axis) and 2C1 (*y*-axis) immunoreactivity in MEF mock-transfected (first panel), expressing ATZ-HA (second panel) or NHK-HA (third panel). HA/2C1 double staining is revealed only in ATZ-HA-expressing cells. Same as panel 2 in CST-treated and in *Cnx*KO MEFs (fourth and fifth panels, respectively).

B Control of ATZ-HA (lane 2) and NHK-HA (lane 3) expression by WB with anti-HA antibodies (upper panel). Loading control (lower panel).

C CLSM analyses showing distribution of the ERAD substrate NHK in WT MEF (upper panels). On BafA1 treatment (lower panels), NHK does not accumulate in LAMP1-positive endolysosomes. Scale bars: 10 μm.

Source data are available online for this figure.

© 2018 The Authors

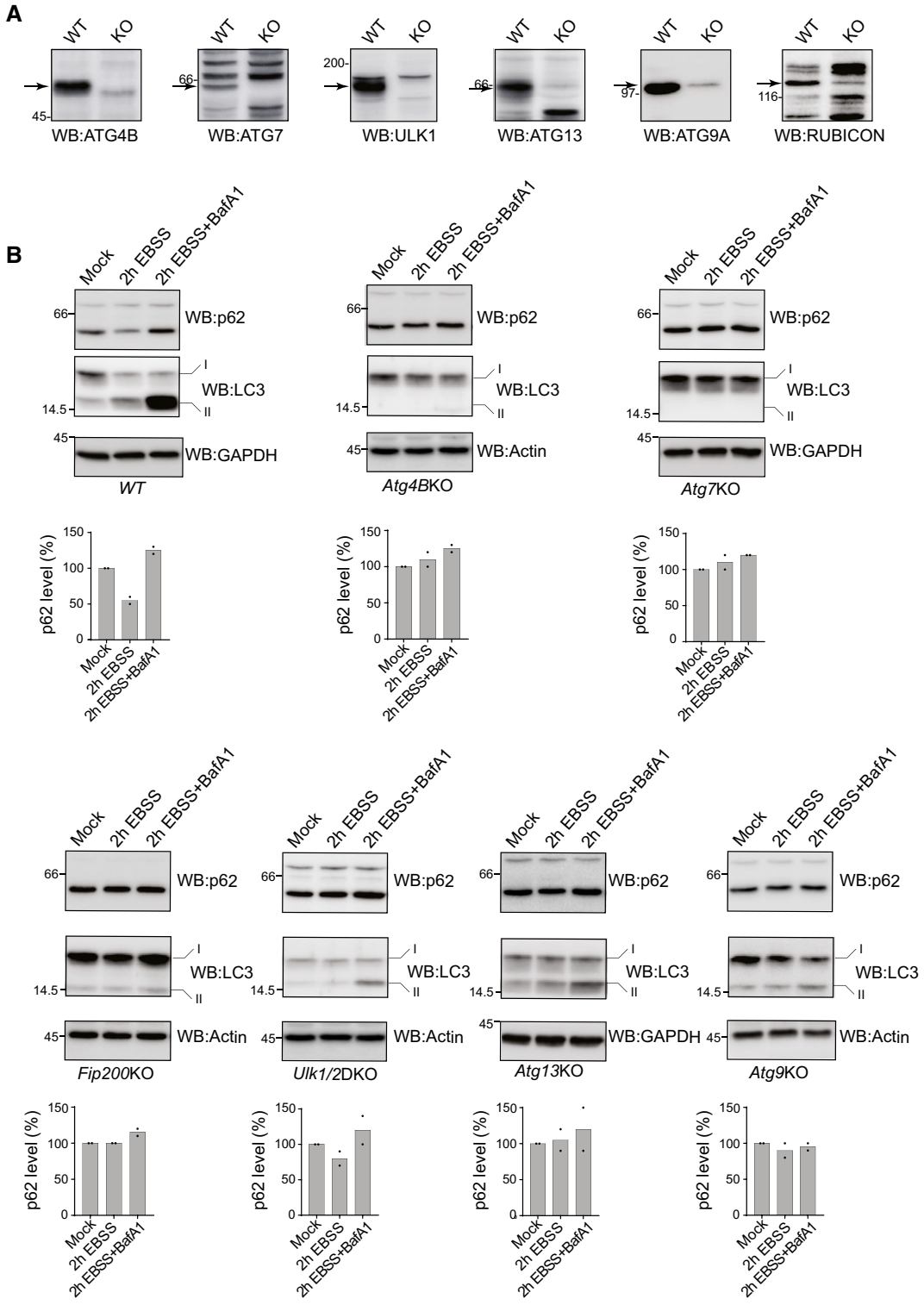

Figure EV3. Macroautophagy activity in *Atg*KO cell lines used in the study.

A KO efficiencies were controlled for ATG4B, ATG7, ULK1, ATG13, ATG9A, and RUBICON (arrows).

B Macroautophagy activity on nutrient deprivation is assessed by monitoring variation of the levels of the macroautophagy substrate p62 by WB in WT, *Atg4*BKO, *Atg7*KO, *Fip200*KO *Ulk1/2*DKO, *Atg13*KO, *Atg9*KO MEFs (the values for two independent experiments are given). For each cell line, also LC3 levels are shown. All the controls performed in this figure confirm the results published by the groups sharing these cell lines (cited in the text and in the Acknowledgements section).

Source data are available online for this figure.

 © 2018 The Authors

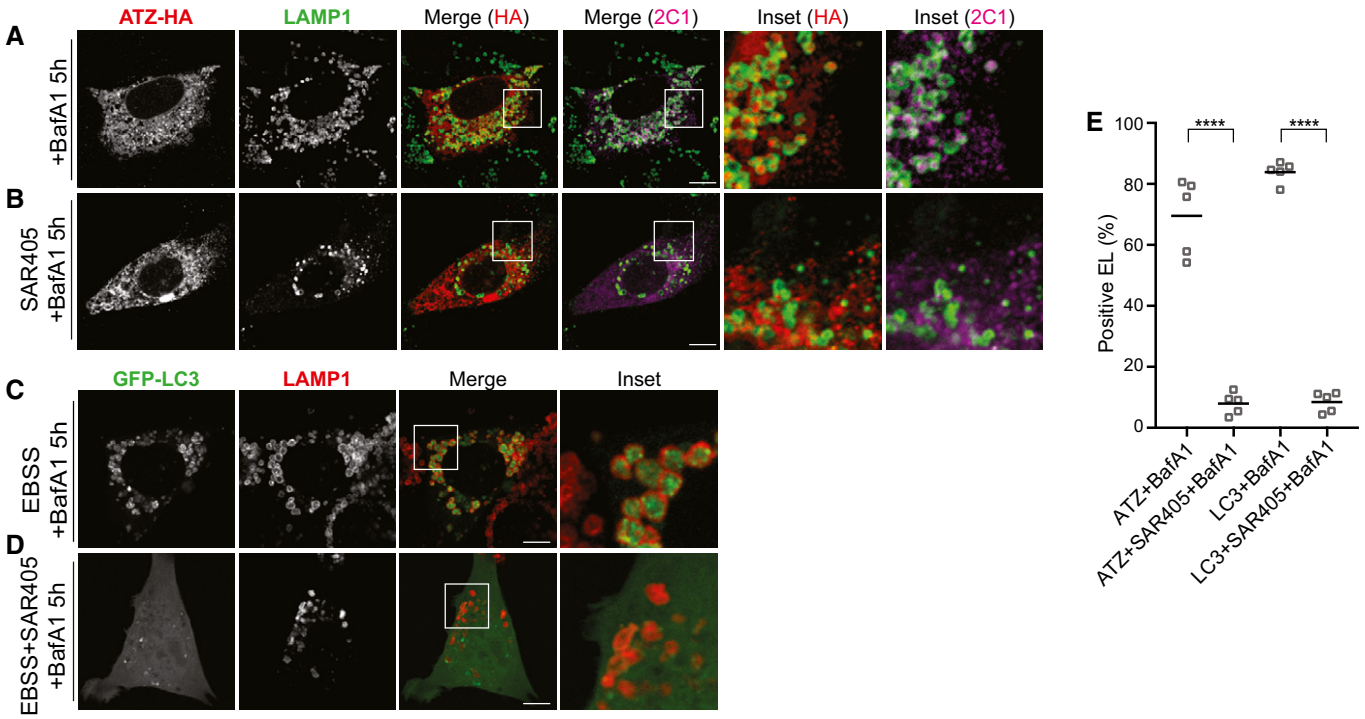

Figure EV4. VPS34 is required for polymeric ATZ delivery to EL.

A, B Intracellular localization of total (HA) and polymeric ATZ (2C1) in WT MEF exposed to 100 nM BafA1 for 5 h and in cells exposed to 5 μM Sar405 and 100 nM BafA1 for 5 h, respectively.

C, D As control for Sar405 treatment, WT MEF transfected with GFP-LC3 were treated as in (A and B), respectively, on nutrient deprivation.

E Quantification of ATZ- or GFP-LC3-positive endolysosomes as shown in (A–D) (n = 5). Unpaired two-tailed t-test, ****$P < 0.0001$.

Data information: Scale bars: 10 μm.

Figure EV5. Various controls.

A Kinetics of total (upper panel) and of polymeric (lower panel, IP:2C1) TMR ligand-labeled HaloTag-ATZ clearance in mock- (lanes 2–6) and in BafA1-treated HEK293 cells (lanes 7–10). Quantification, n = 3 for 30', 180', 300', 300'+BafA1. Mean ± SEM.

B–D CLSM analyses of BafA1-treated WT cells showing co-localization of ATZ-HA (red) and sfGFP-KDEL (green) in LAMP1-positive (cyan) endolysosomes (Inset HA/GFP-KDEL) (B); same in cells expressing only sfGFP-KDEL (C) and in cells co-expressing NHK-HA and sfGFP-KDEL (D). Scale bars: 10 μm. A time course is shown in Fig 6A and B.

E, F Delivery of the endogenous ER-phagy marker CLIMP63 within LAMP1-positive endolysosomes in WT and in CRISPR17 MEF, respectively, exposed to BafA1 on nutrient deprivation. Scale bars: 10 μm.

G Quantification of (E, F) (n = 15, 10 cells). Unpaired two-tailed t-test, $^{ns}P > 0.05$, ****$P < 0.0001$).

H GFP reconstitution in ATZ-HA-transfected CRISPR17 MEF expressing FAM134B-T_{11} and non-lipidable $GFP_{1–10}$-LC3I. Scale bar: 10 μm.

Source data are available online for this figure.

© 2018 The Authors

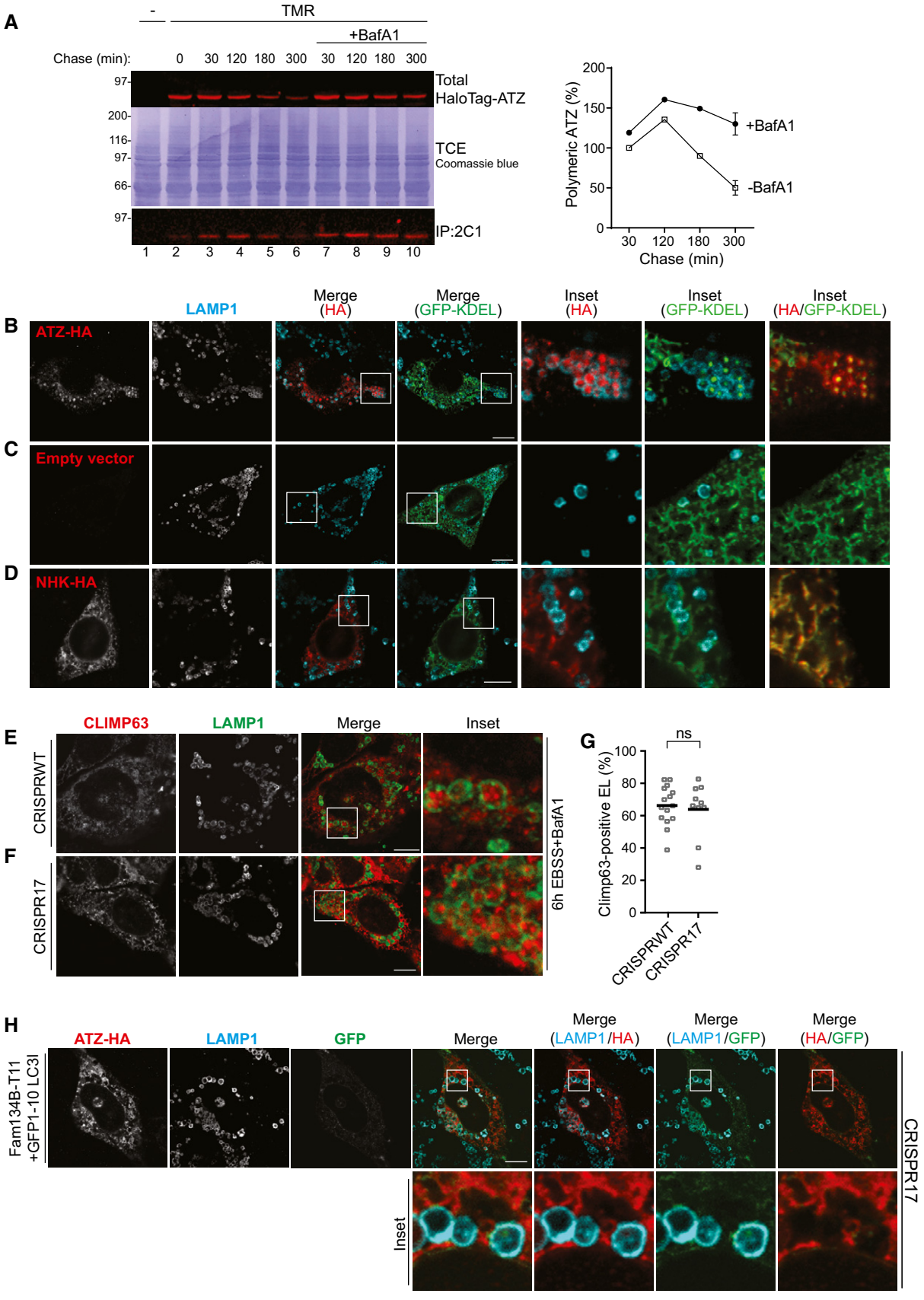

Figure EV5.

© 2018 The Authors